Food Hydrocolloids 176 (2026) 112534

Contents lists available at ScienceDirect

Food Hydrocolloids

journal homepage: www.elsevier.com/locate/foodhyd

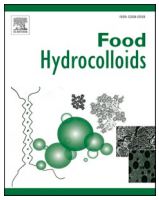

Pelagic *Sargassum* as a sustainable source of food-grade alginate: selective functional modulation by high-pressure processing and sonication

Aravind Kumar Bingi [a], Yaqi Zhao [a], Yu-Jou Chou [a], Chunya Tang [a], Banghao Chen [b], Jeremy D. Owens [c], Brian E. Lapointe [d], Rachel A. Brewton [d], Imran Ahmad [e], Qinchun Rao [a,*]

[a] Department of Health, Nutrition, and Food Sciences, Florida State University, Tallahassee, FL, USA
[b] Department of Chemistry and Biochemistry, Florida State University, Tallahassee, FL, USA
[c] Department of Earth, Ocean, and Atmospheric Science and National High Magnetic Field Laboratory, Florida State University, Tallahassee, FL, USA
[d] Harbor Branch Oceanographic Institute, Florida Atlantic University, Fort Pierce, FL, USA
[e] Chaplin School of Hospitality & Tourism Management, Florida International University, Miami, FL, USA

ARTICLE INFO

Keywords:
Pelagic *sargassum*
Sodium alginate
Response surface methodology
Non-thermal processing

ABSTRACT

Pelagic *Sargassum* spp. represent an abundant and underutilized biomass, and converting this material into functional sodium alginate offers a sustainable pathway for its industrial valorization and food-hydrocolloid applications. This study evaluated the impacts of thermal (autoclave) and non-thermal (high-pressure processing (HPP), sonication) pretreatments on the structural and functional properties of sodium alginate extracted under optimized alkaline conditions (80 °C, 5 h, 0.3 M Na_2CO_3 concentration). To our knowledge, this is the first systematic comparison of thermal and non-thermal pretreatments on the physicochemical and functional characteristics of sodium alginate from pelagic *Sargassum*. Physicochemical properties (yield, molecular weight, viscosity, and monomer composition), structural characterization by Fourier Transform Infrared (FTIR) spectroscopy and proton nuclear magnetic resonance (^{1}H NMR), and functional properties (gel strength and emulsification index) were analyzed to elucidate structure-function relationships. Autoclave pretreatment caused pronounced degradation, resulting in reduced molecular weight (<15 kDa), intrinsic viscosity (<0.35 dL/g), gel strength (77 g), and emulsification capacity (5-6%). In contrast, the non-thermal pretreatments selectively retained functional properties: sonication (10 min) produced the highest gel strength among treated samples (174 g), whereas HPP (400 MPa) produced the highest emulsification index (17.2%). The control exhibited the highest molecular integrity, and similar FTIR and ^{1}H NMR spectra across samples indicated that the alginate backbone remained chemically stable despite partial depolymerization. Overall, the selective improvements observed with HPP and sonication demonstrate that tailored pretreatments can modulate alginate functionality without compromising chemical integrity. These findings highlight a promising strategy to valorize pelagic *Sargassum* by producing functional alginate suitable for clean-label hydrocolloid applications.

1. Introduction

Brown algal blooms, particularly pelagic *Sargassum* species (*S. natans* and *S. fluitans*), have increased dramatically in the North Atlantic Ocean since 2011 (Gower et al., 2013). These accumulations extend across the wider Great Atlantic *Sargassum* Belt, affecting the Caribbean Sea, Gulf of Mexico, and West African coasts, where they create significant environmental and economic challenges (Lapointe et al., 2025; Smetacek & Zingone, 2013). Despite these impacts, their abundance also presents an opportunity for sustainable utilization, similar to other commercially exploited brown seaweeds such as *Saccharina latissima* (Sæther et al., 2024) and *Laminaria digitata* (Purcell-Meyerink et al., 2021). To evaluate this potential, understanding the chemical composition of pelagic *Sargassum* is essential. Biomass collected across the Caribbean and nearby regions shows substantial variation in proximate composition, mineral content, and trace elements depending on location and season (Table 1). Even with this variability, it consistently contains high levels of essential minerals, reinforcing its promise as a sustainable raw material.

A promising route for valorizing pelagic *Sargassum* lies in extracting

* Corresponding author.
E-mail address: qrao@fsu.edu (Q. Rao).

https://doi.org/10.1016/j.foodhyd.2026.112534
Received 5 December 2025; Received in revised form 20 January 2026; Accepted 5 February 2026
Available online 6 February 2026

high-value polysaccharides such as alginate, which constitutes up to 21.0% of the dry weight (DW, Table 1) and serves as a major structural component in brown algal cell walls (Jung et al., 2013). Alginate is a linear copolymer composed of α-L-guluronic acid (G) and β-D-mannuronic acid (M), with its functional properties largely dictated by the G/M composition and block distribution (Skjåk-Bræk et al., 1989). Owing to its gelling, thickening, and emulsifying properties, sodium alginate is widely used in food applications, including ice cream, dairy formulations, and salad dressings (Pournaki et al., 2024).

However, despite its polysaccharide richness, pelagic *Sargassum* can accumulate heavy metals such as arsenic, lead, and cadmium, which raises safety concerns for the direct use of raw biomass in food applications (Liranzo-Gómez et al., 2023). Published chemical profiling studies across the Caribbean and Atlantic regions (Table 1) further show

Table 1
Proximate composition, alginate content, mineral profile, and toxic element concentrations of pelagic *Sargassum* collected across different geographic locations and seasons. M.-C. Lee et al. (2023); Tonon et al. (2022); Bauta et al. (2024); Rodríguez-Rodríguez et al. (2025); Vázquez-Delfín et al. (2021); Melchor-Martínez et al. (2023); Chikani-Cabrera et al. (2022); Olguin-Maciel et al. (2022); Leal-Bautista et al. (2024); Canul-Ku et al. (2023); Salgado-Hernández, Alvarado-Lassman et al. (2023); Salgado-Hernández, Ortiz-Ceballos, et al. (2023); Milledge et al. (2020); Nielsen et al. (2021); GraphPad, (2025).

Country	Sampling			Proximates (g/100 g DW)										Minerals (mg/kg DW)																References
	Time	Location	Coordinates	Moisture	Protein	Lipid	Fatty acids % of TFA				Ash	Total solids	Volatile solids	Alginate	Essential minerals																
							MUFA	PUFA	SFA	UFA					Macrominerals					Microminerals						Toxic elements						
															Ca	Mg	P	K	Na	Cr	Cu	Fe	Mn	Zn	Ni	Al	As	Cd	Pb	Hg	Ba	
Belize	Oct-22	-	-	-	-	-	-	-	-	-	-	-	-	-	-	-	-	-	-	-	-	-	-	-	-	-	84,1	0,4	0,1	ND	-	M.-C. Lee et al. (2023)
Dominican Republic	Feb-21	Municipality of Higuey	-	18,8	-	-	28,8	18,1	33,1	20,1	16,6	81,2	-	2,5	41,717	6,553	-	18,939	7,383	2,0	3,5	58,8	14,5	13,7	4,4	28,5	21,4	0,4	0,5	-	26,9	Tonon et al. (2022)
	Oct-21	Punta Cana	-	16.7	6.2	0.5	28.2	22.3	49.4	-	15.5	83.3		25.8	44,315	8,229			13,182	0.6	4.4			6.7	5.8		48.3	0.7	0.2	0.01	-	Bauta et al. (2024)
	Oct-22	Punta Cana	18°32'23.83"N 68°21'15,02"W	-	5.4	1.0	-	-	-	-	-	-	-	-	12,448	4,723	275	1,016	10,847	3,1	2,4	42,0	-	2,0	2,8	10,0	61,6	0,3	0,1	0,05†	10,7	Rodríguez-Rodríguez et al. (2025)
Guadeloupe (France)	Jun-21	Vieux Habitants	-	15,2	6,4	0,6	24,7	7,4	67,9	-	14,8	84,8	-	25,5	62,398	11,244	-	-	5,528	0,9	10,7†	-	-	59,4	4,5	-	16,8	0,7	0,4	0,01	-	Bauta et al. (2024)
	Sep-21	Le Gosier	-	17,8	6,6	0,8	24,1	4,5	71,4	-	16,2	82,2	-	23,1	55,616	10,010	-	-	7,819	0,6	4,1	-	-	3,7	5,3	-	53,2	0,6	0,7	0,01	-	
	Jan-22	Bouillante	-	17,4	7,7	0,3	17,0	12,2	71,8	-	19,9	82,6	-	30,2	63,698	11,802	-	-	6,835	0,9	9,8	-	-	47,7	5,1	-	17,6	0,8	0,5	0,01	-	
	Jul-22	Saint-Félix seaport	-	13,8	6,3	1,1	23,1	10,6	66,3	-	14,5	86,2	-	17,8	43,208	8,991	-	-	9,066	2,2	4,2	-	-	5,3	6,6	-	86,0	0,8	0,4	0,01	-	
Jamaica	Feb-19	Hellshire Bay	-	8,2	-	-	-	-	-	-	34,1	91,8	-	13,5-	-	-	-	-	-	-	-	-	-	-	-	-	-	-	-	-	Tonon et al. (2022)
	Aug-20	Hellshire Bay	-	8.5	-	-	21.8	12.3	44.1	21.8	37.0	91.5	-	7.0	34,476	8,307	-	56,013	30,804	1.5	2.1	53.4	22.3	3.9	3.8	62.8	86.8	0.4	0.9	-	15.2	
Marie-Galante (France)	Jun-22	Plage des Galets	-	13,4	5,2	0,8	24,6	13,0	62,4	-	15,9	86,6	-	18,4	51,198	12,455	-	-	11,917	0,7	3,4	-	-	9,5	5,4	-	54,2	0,6	0,9	0,005	-	Bauta et al. (2024)
		Capesterre	-	14,1	7,3	0,8	18,6	9,5	71,9	-	17,8	85,9	-	18,5	59,929	11,291	-	-	8,518	0,6	2,4	-	-	3,1	4,2	-	17,8	0,9	0,5	0,01	-	
Mexico	Sep-18	Playa Mirador	20°10'19,4"N 87°26'54,7"W	83,2*	9,9	2,5	-	-	-	-	23,9	-	-	29,8	-	-	-	-	-	-	0,6	31,5	-	3,7	-	-	65,7	0,6	0,2	-	-	Vázquez-Delfín et al. (2021)
		Playa Blanca	20°24'15,5"N 87°18'33,5"W	83,8*	10,1	3,0	-	-	-	-	23,7	-	-	32,1	-	-	-	-	-	-	0,2	24,0	-	4,0	-	-	40,5	1,3	0,2	-	-	
		Playa Xcalacoco	20°39'43,0"N 87°01'55,4"W	84,4*	10,3	3,0	-	-	-	-	21,9	-	-	29,3	-	-	-	-	-	-	0,3	54,6	-	5,8	-	-	43,2	0,8	0,2	-	-	
		Puerto Morelos	20°50'44,1"N 86°52'35,5"W	86,0*	9,8	2,7	-	-	-	-	18,1	-	-	33,9	-	-	-	-	-	-	0,6	31,0	-	3,6	-	-	41,1	1,4	0,2	-	-	
		Playa Coral	21°01'29,4"N 86°48'43,9"W	84,3*	8,3	3,4	-	-	-	-	19,2	-	-	32,7	-	-	-	-	-	-	0,9	28,7	-	7,2	-	-	29,0	1,2	0,2	-	-	
		Playa Delfines	21°03'43,3"N 86°46'41,7"W	83,0*	8,1	3,3	-	-	-	-	20,7	-	-	30,5	-	-	-	-	-	-	1,1	25,9	-	5,0	-	-	64,9	0,3	0,3	-	-	
	Jan-20	Punta Sur	20°17'57,0"N 87°00'22,0"W		13,6	2,8	-	-	-	-	11,3	-	-	-	-	-	-	-	-	-	-	-	-	-	-	-	-	-	-	-	Melchor-Martínez et al. (2023)
	Jul-20	Cancún	-	11,8	-	-	20,8	12,6	41,4	25,2	58,6	88,2	-	1,4	24,199	7,424	-	34,178	32,368	0.7	2.4	45.3	11.0	4.8	4.6	10.8	55.9	0.4	0.5	-	22.6	Tonon et al. (2022)
	Sep-20 to Sep-21	Puerto Morelos	20°50'55,17"N 86°52'34,46"W	13,0	-	-	-	-	-	-	22,2	87,0	77,8	-	-	-	-	-	-	-	-	-	-	-	-	-	-	-	-	-	Chikani-Cabrera et al. (2022)
	Sep-20	Puerto Morelos	-	86,2*	-	-	-	-	-	-	22,6	-	-	-	-	-	-	-	-	-	1,3	18,7	15,2	8,8	1,9	10,2	76,9	ND	ND	-	-	Olguin-Maciel et al. (2022)
	Jan-21	Puerto Morelos	-	13,6	-	-	24,1	14,1	33,5	28,2	30,1	86,4	-	6,6	36,895	8,575	-	48,214	36,705	0,7	2,3	47,9	13,6	11,5	4,7	19,1	53,9	0,8	3,1†	-	19,6	Tonon et al. (2022)
	Feb-21	California Beach	24°15'37"N 110°36'49"W	-	6,5	2,5	-	-	-	-	14,7	-	-	-	-	-	-	-	-	-	-	-	-	-	-	-	-	-	-	-	-	Melchor-Martínez et al. (2023)
	May-21	Altamar	-	86,2*	-	-	-	-	-	-	22,6	-	77,4	-	-	-	-	-	-	-	-	-	-	-	-	-	-	-	-	-	-	Leal-Bautista et al. (2024)
		Antes de Barrera	-	85,7*	-	-	-	-	-	-	27,1	-	73,0	-	-	-	-	-	-	-	-	-	-	-	-	-	-	-	-	-	-	
		Después de Barrera	-	83,7*	-	-	-	-	-	-	19,5	-	80,5	-	-	-	-	-	-	-	-	-	-	-	-	-	-	-	-	-	-	
		Playa	-	80,6*	-	-	-	-	-	-	20,9	-	78,7	-	-	-	-	-	-	-	-	-	-	-	-	-	-	-	-	-	-	
	Sep-21	San Miguelito Beach	-	12,2	6,7	-	-	-	-	-	40,1	87,8	-	-	88,730	0,0	0,0	285,700†	1,800	ND	0,0	1,600	100†	15,900†	-	500†	530	ND	ND	ND	-	Canul-Ku et al. (2023)
	-	Playa del Carmen	20°37'19.99"N 87°4'9.98"W	10.0	-	-	-	-	-	-	44.2	90.0	44.7	-	74,800	7,700	-	10,900	32,000	-	-	-	-	-	-	-	-	-	-	-	-	Salgado-Hernández, Alvarado-Lassman, et al. (2023)
	-	Playa del Carmen	20°37'25.1"N 87°04'23.6"W	80.3*	-	-	-	-	-	-	6.4	-	13.2	-	93,000	8,100	-	7,300	7,900	-	-	-	-	-	-	-	-	-	-	-	-	Salgado-Hernández, Ortiz-Ceballos, et al. (2023)
Saint Lucia	Oct-22	-	-	-	-	-	-	-	-	-	-	-	-	-	-	-	-	-	-	-	-	-	-	-	-	-	109	0,4	0,03	ND	-	M.-C. Lee et al. (2023)
Saint Vincent and the Grenadines	-		-	-	-	-	-	-	-	-	-	-	-	-	-	-	-	-	-	-	-	-	-	-	-	-	111	0,4	0,1	ND	-	
Saint Kittis and Nevis	-		-	-	-	-	-	-	-	-	-	-	-	-	-	-	-	-	-	-	-	-	-	-	-	-	106	0,3	ND	ND	-	
Turks and Caicos	Jun-19	South Caicos	21°29'27,6"N 71°30'10,8"W	82,0*	-	3,9	19,3	29,3	36,7	14,7	46,9	-	9,6	-	70,306	12,053	501	69,359	-	0,3	2,5	3,811†	30,2	5,8	-	37,5	124	0,1	0,3	0,01	-	Milledge et al. (2020)
	Sep-20 to May-21	South Caicos	21°29'27,6"N 71°30'10,8"W		-	-	-	-	-		38,2	-	61,8	-	-	-	-	-	-	0,004 -1,0 -		-	-	-	-	15,8 - 50,1	63,1 - 175	0,1 - 0,2	ND - 0,5	-	-	Nielsen et al. (2021)
USA	Jun-24	Miami	27°27'23,0"N 80°05'36,0"W	14,4	-	-	-	-	-			85,6	-	20,0	-	-	-	-	-	-	-	-	-	-	-	-	-	0,5	ND	-	-	This study
Average				**13.7**	**7.9**	**1.9**	**22.9**	**13.8**	**54.2**		**24.4**	**86.3**	**63.4**	**21.0**	**53,558**	**9,164**	**388**	**30,740**	**14,845**	**1.1**	**2.6**	**159**	**17.8**	**11**	**4.5**	**25.6**	**80.0**	**0.6**	**0.4**	**0.01**	**19.0**	

* g/100 g, wet weight
† Identified as a significant outlier ($P < 0.05$) (GraphPad, 2025) and excluded from the average calculation.
DW: Dry weight; ND:Not detected
MUFA: Monounsaturated fatty acids; PUFA: Polyunsaturated fatty acids; SFA: Saturated fatty acids; UFA: Unidentified fatty acids
Al: Aluminum; As: Arsenic; Ba: Barium; Cd: Cadmium; Cr: Chromium; Cu: Copper; Fe: Iron; Hg: Mercury; K: Potassium; Mg: Magnesium; Mn: Manganese; Na: Sodium; Ni: Nickle; Pb: Lead; P: Phosphorus; Zn: Zinc

substantial spatial and seasonal variability in proximate composition and toxic element content, highlighting the need for controlled processing. Selective extraction and purification of polysaccharides such as alginate can reduce metal co-extraction while preserving functional integrity, and these processes can also yield purified fractions enriched in bioactive components with lower heavy-metal burdens, supporting the development of value-added seaweed-derived ingredients (Cherry et al., 2019).

Traditional alginate extraction involves an acid pretreatment to remove multivalent counterions, followed by alkaline solubilization using sodium carbonate or sodium bicarbonate. This step converts the insoluble alginic acid present in the seaweed cell walls into the water-soluble sodium alginate form, which is then precipitated using ethanol or calcium chloride (Pawar & Edgar, 2012). In recent years, advanced processing techniques such as microwave-assisted extraction (Yuan & Macquarrie, 2015), pressurized liquid extraction (Saravana et al., 2018), enzyme-assisted extraction (Rostami et al., 2017), and supercritical fluid extraction (Balboa et al., 2015) have been explored to improve extraction efficiency. However, these approaches may face barriers to industrial implementation due to scale-up limitations, added costs/complexity, and potential polymer degradation under harsh or poorly controlled conditions (Bojorges, López-Rubio et al., 2023).

Alternatively, thermal and non-thermal pretreatments, such as autoclaving, high-pressure processing (HPP), and sonication, represent practical, food-grade technologies already established in the food industry. These processes can alter the polymer structure through heat, pressure, or cavitation, which may influence the efficiency and functionality of sodium alginate extraction. Importantly, by modulating chain length, flexibility, and entanglement, HPP and sonication may enable directional functional tuning of alginate performance, rather than simply maximizing yield. These methods operate through distinct mechanisms: autoclaving employs high heat and pressure to induce polymer breakdown; HPP applies isostatic pressure without heat, promoting structural rearrangements; and sonication causes mechanical disruption via cavitation (Andreou et al., 2017). Although these methods have been shown to alter molecular weight, viscosity, and gelation behavior in various biopolymers (Din et al., 2019; Tsikrika et al., 2021), their specific effects on sodium alginate extraction from *Sargassum* spp. remain underexplored. As mentioned above, understanding how these pretreatments affect the structure and functionality of sodium alginate is essential for developing scalable strategies to optimize its application in food systems.

This study investigates the comparative effects of autoclave, HPP, and sonication on the physicochemical and functional properties of sodium alginate extracted from pelagic *Sargassum* spp., enabling the tailored design of sodium alginate with desired gelation and emulsification characteristics. By identifying application-specific processing strategies, these findings support the industrial valorization of *Sargassum*-derived sodium alginate for use in food products, hydrocolloids, and other functional ingredients. Heavy metal analysis of the source biomass provides a safety-relevant context, and the extraction and purification workflow applied here is expected to reduce inorganic contaminants relative to the raw material.

2. Materials and methods

All chemicals and reagents were of analytical grade. All solutions were prepared using deionized (DI) water (18.2 MΩ cm), obtained through a 0.2-μm filter using a NANOpure DIamond water purification system (Barnstead International, Inc., Dubuque, IA, USA).

2.1. Pelagic Sargassum sampling

Pelagic *Sargassum* used in this study was obtained from two sources: a beach-collected sample and an ocean-harvested sample. The beach-collected material, hand-gathered during a seasonal influx in May 2023 from the shoreline of Miami Beach, FL, USA (two collection access points: 25°59′58.5″N, 80°06′57.8″W and 26°06′49.9″N, 80°06′14.5″W), was used to optimize alkaline extraction conditions. In contrast, the ocean-harvested sample, collected from floating mats offshore in June 2024 (27°27′23.0″N, 80°05′36.0″W), was employed for all subsequent pretreatment and characterization experiments to ensure compositional uniformity and minimize contamination from sand and debris. For both types, fresh samples were immediately transferred into sealed polyethylene bags and stored in an insulated container with ice packs. Desalting was carried out within 12 h based on Contreras et al. (2008) with modifications. Briefly, about 2 kg of fresh biomass was washed 10 times with 15 L of DI water at room temperature (RT) to remove surface salts, epiphytes, and loosely associated marine fauna. After desalting, the seaweed was gently blotted dry using paper towels, freeze-dried (Labconco Corporation, Kansas City, MO, USA), and pulverized. The resulting dried *Sargassum* powder was stored at −20 °C in airtight containers for further use. Basic characteristics of the two biomasses (moisture/dry matter and purified alginate yield on a dry-weight basis) are provided in Supplementary Material (Table S1).

2.2. Heavy metal analysis

One gram of ocean-harvested *Sargassum* powder was transferred into a Teflon digestion vessel and subjected to microwave-assisted acid digestion in a trace-metal clean laboratory using a MARS-6 Microwave Digestion System (CEM Co., Matthews, NC, USA). 10 mL of double-distilled, trace-metal-grade concentrated HNO_3 was added to the sample for overnight pre-digestion. Then, the sample was digested at 210 °C for 15 min. The concentrations of trace metals, cadmium (Cd), and lead (Pb) in the digested seaweed biomass were determined using a 225ATS Atomic Absorption Spectrometer (AAS, Buck Scientific Instruments, LLC., Ansonia, CT, USA) and expressed as mean ± standard error of the mean (SEM). The instrument was calibrated using standard solutions containing 1000 ppm of each metal in 2% (v/v) HNO_3 (Absolute Standards, Inc., Hamden, CT, USA).

2.3. Sodium alginate extraction

Four sample groups were prepared: a control (no pretreatment) and three pretreatments, autoclaving, HPP, and sonication. Pretreatment conditions were selected based on representative parameter ranges reported in prior literature and adjusted to match equipment operating limits (Table S2). For all groups, the *Sargassum* powder was first mixed with DI water at a solid-to-liquid ratio of 1:60 (w/v). For the autoclave pretreatment, the hydrated *Sargassum* was transferred to an autoclavable glass bottle and heated at 121 °C and 35 psi for 10 min and 30 min using a Harvey Sterilemax (Barnstead Thermolyne Corporation, Dubuque, IA, USA). For the HPP pretreatment, the hydrated powder was placed in an HPP-compatible polyethylene bottle and processed at 400 MPa and 600 MPa for 10 min at RT using the Hiperbaric 55 system (Hiperbaric USA Corporation, Miami, FL, USA). For the sonication pretreatment, the hydrated powder was treated in an ultrasonic bath (Branson CPX 8800, Branson Ultrasonics, Brookfield, CT, USA) at 40 kHz for 10 min and 30 min at RT. Following pretreatment, sodium alginate was extracted through four successive steps: acid treatment, alkali extraction, bleaching, and purification.

2.3.1. Acid treatment

Acid treatment was performed according to Hernández-Carmona et al. (1999) with modifications. Briefly, 0.2 M HCl was added at a solid-to-liquid ratio of 1:25 (w/v) and stirred overnight at RT. The residue was then recovered by centrifugation (3,000*g* for 15 min at RT) and subjected to alkali extraction.

2.3.2. Alkali extraction

The alkali extraction process was optimized using response surface

methodology based on the Box-Behnken Design (RSM-BBD). This approach was employed to evaluate the influence of extraction parameters on crude sodium alginate yield, calculated using Eq. (1). Three independent uncoded variables were considered: temperature (A, 40-80 °C), extraction time (B, 1-5 h), and sodium carbonate (Na_2CO_3) concentration (C, 0.1-0.3 M). The extraction was performed at a fixed solid-to-liquid ratio of 1:50 (w/v). Each variable was evaluated at three coded levels (−1, 0, +1), as shown in Table 2. The BBD is a widely used three-level RSM design for efficient quadratic modeling with a limited number of experimental runs. Replicated centre points were included to estimate pure error and assess model adequacy (lack-of-fit). The design enabled the development of a second-order polynomial model and the analysis of factor interactions influencing yield.

$$\text{Crude yield}\ (\%) = \frac{\text{Mass of crude alginate}}{\text{Mass of seaweed used for extraction}} \times 100 \qquad \text{Eq. 1}$$

2.3.3. Bleaching and purification

The crude sodium alginate was bleached by adding 5% (v/v) sodium hypochlorite and stirring for 20 min at RT. The bleached extract underwent purification according to McHugh et al. (2001) with modifications. Briefly, 1 M HCl was added until the pH reached 2, converting soluble sodium alginate into insoluble alginic acid. The precipitate was collected by centrifugation (3,000*g* for 15 min at RT). The alginic acid was mixed with 15 mL of 95% (v/v) ethanol and stirred for 2 h at RT. Then, 5% (w/v) Na_2CO_3 was added until the pH reached 10, forming a thick sodium alginate gel. This gel was recovered by centrifugation and subsequently freeze-dried. The yield of purified sodium alginate was calculated using Eq. (2).

$$\text{Purified yield}\ (\%) = \frac{\text{Mass of purified alginate}}{\text{Mass of seaweed used for extraction}} \times 100 \qquad \text{Eq. 2}$$

2.4. Characterization of extracted sodium alginate

2.4.1. Fourier transform infrared (FTIR) spectroscopy

Infrared (IR) spectra of sodium alginate powder were obtained using a JASCO FT/IR-6800 spectrometer (JASCO Corporation, Easton, MD, USA) equipped with a universal attenuated total reflectance (ATR) accessory for direct sample analysis with minimal preparation. Spectra were recorded at room temperature over the range of 6000-250 cm^{-1} with a resolution of 4 cm^{-1}, averaging 64 scans per spectrum. The resulting data were analyzed to assess the chemical composition and structure of the sodium alginate samples using OriginPro (version 2025, OriginLab Corporation, Northampton, MA, USA).

Table 2
Box-Behnken Design with coded and uncoded variables (A: Temperature, B: Extraction time, C: Na_2CO_3 Concentration) and results of the observed response (Crude yield).

Run	Independent variables			Response
	Temperature (A) (°C)	Extraction time (B) (h)	Na_2CO_3 Concentration (C) (M)	Crude yield (%)
1	40 (−1)	1 (−1)	0.2 (0)	16.26
2	80 (+1)	1 (−1)	0.2 (0)	26.61
3	40 (−1)	5 (+1)	0.2 (0)	24.72
4	80 (+1)	5 (+1)	0.2 (0)	41.16
5	40 (−1)	3 (0)	0.1 (−1)	21.67
6	80 (+1)	3 (0)	0.1 (−1)	34.88
7	40 (−1)	3 (0)	0.3 (+1)	29.06
8	80 (+1)	3 (0)	0.3 (+1)	41.29
9	60 (0)	1 (−1)	0.1 (−1)	16.02
10	60 (0)	5 (+1)	0.1 (−1)	27.30
11	60 (0)	1 (−1)	0.3 (+1)	22.72
12	60 (0)	5 (+1)	0.3 (+1)	37.41
13	60 (0)	3 (0)	0.2 (0)	29.66
14	60 (0)	3 (0)	0.2 (0)	30.40
15	60 (0)	3 (0)	0.2 (0)	29.25

2.4.2. Nuclear magnetic resonance (NMR)

The M/G ratio of sodium alginate was determined using ^1H NMR spectroscopy according to ASTM-F2259-10 (2012). Sodium alginate solutions (0.1%, w/v) were prepared in 99.9% D_2O and partially hydrolyzed by acid treatment. The pH was adjusted to 5.6 using 0.1 M HCl, and the samples were heated in a water bath at 100 °C for 1 h. After cooling to RT, the pH was further adjusted to 3.8 with 0.1 M HCl and reheated in the water bath at 100 °C for 30 min. Hydrolysis was stopped by placing the samples on ice. The solution was neutralized to pH 7 using 0.1 M sodium hydroxide and lyophilized overnight. The freeze-dried sodium alginate was dissolved in 1 mL of 99.9% D_2O and freeze-dried again. A final aliquot of 10-12 mg of the powder was dissolved in 1 mL of 99.9% D_2O and transferred to an NMR tube along with 20 μL of 0.3 M Triethylenetetramine-N,N,N′,N″,N‴,N⁗-hexaacetic acid as a chelating agent.

The ^1H NMR spectra were recorded at 80 °C on a Bruker AVIII 500 MHz NMR spectrometer (Bruker Corporation, Billerica, MA, USA) with a 5-mm TXI probe. The ^1H Larmor frequency is 500.13 MHz. Each spectrum was obtained with 64 scans and a 1-s recycle delay. Spectral data were processed using MestReNova 14.2.1 software (Mestrelab Research S.L., Santiago de Compostela, Spain).

2.5. Physicochemical and functional property analyses

2.5.1. Apparent viscosity

Sodium alginate solutions (0.25%, w/v) were prepared by dissolving the samples in DI water and stirring at RT for at least 4 h. The apparent viscosities of sodium alginate extracted from pretreated *Sargassum* were measured using a DV3TLV cone-plate viscometer (Brookfield Engineering Laboratories, Inc., Middleboro, MA, USA) equipped with a CPA-40Z spindle. Measurements were conducted at RT across a spindle speed range of 1-25 rpm with a gap of 13 μm.

2.5.2. Viscosity-average molecular weight

Sodium alginate solutions (0.05-0.3 g/dL) were prepared in 0.1 M NaCl. The viscosity-average molecular weight (M_v) was determined using intrinsic viscosity measurements, as described by Torres et al. (2007) and Chee et al. (2011). Briefly, the intrinsic viscosity ($[\eta]$, dL/g) was measured using a Ubbelohde viscometer with a 0.5 mm capillary diameter (Cat. No. 9721-R65, Cannon Instruments Company, PA, USA). The flow time of the sodium alginate solution (t_n, s) was measured relative to the solvent (0.1 M NaCl) flow time (t_0, s), and the specific viscosity (η_{sp}) was calculated using Eq. (3). The average flow time was recorded as t_n. $[\eta]$ was determined by plotting reduced viscosity ($\frac{\eta_{sp}}{C}$, dL/g) against sodium alginate concentration (C, g/dL), based on the Huggins equation (Eq. (4)), where k_H is the Huggins constant. M_v (g/mol) was then calculated from $[\eta]$ using the Mark-Houwink-Sakurada equation (Eq. (5)).

$$\eta_{sp} = \frac{t_n - t_0}{t_0} \qquad \text{Eq. 3}$$

$$\frac{\eta_{sp}}{C} = k_H[\eta]^2 C + [\eta] \qquad \text{Eq. 4}$$

$$[\eta] = 0.023 \times M_v^{0.0984} \qquad \text{Eq. 5}$$

2.5.3. Gel strength

Sodium alginate gels were prepared using an internal gelation method based on Djemaa et al. (2024) with modifications. Briefly, a 2% (w/v) sodium alginate solution (5 mL) was prepared in DI water and degassed at RT for 15 min at 50 mbar. A calcium-EDTA complex solution (0.08 M) was adjusted to pH 7-8 using 1 M NaOH and then mixed (1:1, v/v) with the degassed sodium alginate solution. Subsequently,

glucono-δ-lactone (1%, w/v) was added and gently rotated until completely dissolved. The mixture was left undisturbed at RT overnight for gel formation. To strengthen the gels, the beaker containing the initial gel was immersed in 1 M $CaCl_2$ solution until complete gelation occurred. Excess surface liquid was gently removed prior to texture analysis. Representative images of the gels prepared using this method are included in Fig. S1.

Gel strength was measured using a TA.XTplus Texture Analyzer (Stable Micro Systems, Godalming, UK) equipped with a TA-212 cylindrical probe (7.94 mm, round end). The instrument was operated in compression mode (4 mm) with a trigger force of 1.0 g. The pre-test, test, and post-test speeds were set at 1.0, 0.5, and 0.5 mm/s, respectively.

2.5.4. Emulsification index

The ability of sodium alginate to stabilize emulsions containing medium-chain triglyceride (MCT) oil was evaluated following Fawzy et al. (2017) with modifications. A 1% (w/v) sodium alginate solution was mixed with MCT oil at a 3:2 (v/v) ratio and homogenized using an IKA T25 ULTRA-TURRAX disperser (IKA Works, Inc., Wilmington, NC, USA) at 11,000 rpm for 1 min. After standing for 24 h at RT, the emulsification index (E_{24}) was calculated using Eq. (6), where H_e (cm) is the height of the emulsion and H_t (cm) is the total height.

$$\textit{Emulsification index}\ (E_{24}) = \frac{H_e}{H_t} \times 100 \qquad \text{Eq. 6}$$

2.6. Statistical analysis

To optimize the alkali extraction process (section 2.3.2), statistical modeling and optimization were carried out using Minitab® Statistical Software 22.4.0 (Minitab, LLC, State College, PA, USA). To study the purity of alginate (section 2.3.3), its M/G ratio (section 2.4.2), and its physicochemical and functional properties (section 2.5), one-way analysis of variance (ANOVA) followed by Dunnett's multiple comparison test was performed to evaluate differences among three pretreatment groups relative to the control using GraphPad Prism version 10.2.2 for Windows (GraphPad Software, LLC, Boston, MA, USA).

Each experiment was conducted at least in duplicate, and the data were presented as mean ± SEM. Differences were considered statistically significant at $P < 0.05$.

3. Results and discussion

3.1. Toxic heavy metals in pelagic Sargassum

The concentrations of Cd and Pb in lyophilized pelagic *Sargassum* powder were quantified to assess the safety of the biomass as a potential source for food-grade alginate. Cd was detected at 0.49 ± 0.08 mg/kg DW, whereas Pb was below the detection limit of the Buck Scientific 225ATS AAS (<0.01 mg/kg DW), indicating minimal Pb contamination. Previous studies have shown that heavy metals in extracted sodium alginate are typically reduced relative to the source biomass and, in some cases, fall below analytical detection limits (Pragatheeswari & Raajeswari, 2024; Ruslan et al., 2019; Y. Zhang et al., 2025). This reduction has been attributed, in part, to demineralization/acid washing and precipitation-reconversion steps that remove inorganic impurities during processing (Díaz-Vázquez et al., 2015). Because the present workflow includes HCl demineralization followed by alginic-acid precipitation and re-neutralization to sodium alginate, the purified product is expected to contain only low residual metal levels consistent with established food-additive specifications.

When compared with published values for pelagic *Sargassum* collected across the Caribbean and Atlantic (Table 1), the Cd concentration observed in this study falls within the reported regional range of 0.1-1.4 mg/kg DW, while Pb remains consistently low or non-detectable across most regions. These differences in Cd and Pb relative to other pelagic *Sargassum* samples are consistent with the strong regional and temporal fluctuations in metal accumulation documented for this biomass, reflecting differences in oceanographic conditions, nutrient loads, and local pollution sources. Beyond Cd and Pb, literature data (Table 1) also show that pelagic *Sargassum* contains other toxic elements, including aluminum (25.6 mg/kg), total arsenic (61.2 mg/kg), and trace mercury (0.01 mg/kg), indicating broader contaminants typically associated with this biomass.

The absence of detectable Pb is particularly noteworthy, as Pb is known for its neurotoxicity, bioaccumulation potential, and the existence of strict regulatory limits in food products (J.-W. Lee et al., 2019; WHO, 2011). According to the Codex Alimentarius Commission (2024), the maximum permissible limits for Cd and Pb in food products range from 0.1 to 2 mg/kg and 0.01-2.5 mg/kg, respectively. Although no international thresholds specifically exist for edible seaweed, the measured values fall within the lower end of these ranges.

In the United States, regulatory limits for Cd and Pb in edible seaweeds or alginate products have not yet been established. The FDA monitors heavy metals in foods and has set action limits for Pb in selected products (e.g., 0.05 mg/kg for fruit juices (FDA, 2018a) and 0.1 mg/kg for candy (FDA, 2018b)). For Cd, the FDA applies a toxicological reference value of 0.21-0.36 μg/kg bodyweight/day (FDA, 2024) for dietary exposure assessment. While these benchmarks do not directly apply to seaweed, they provide context for interpreting the relatively low metal concentrations found in pelagic *Sargassum*.

Recent evaluations of pelagic *Sargassum* emphasize that this biomass is not suited for direct human consumption due to its high salt content, fiber load, and the presence of potentially toxic elements (Carrillo-Domínguez et al., 2023). Instead, its practical applications are currently limited to compost, soil amendments, livestock feed, and pet-food formulations, where inclusion levels below 5% are recommended for safety and performance (Makkar et al., 2016). Accordingly, the primary value of pelagic *Sargassum* lies not in its use as a food but as a raw material for extracting purified hydrocolloids, such as alginate, with potential for food-related applications.

Collectively, the low Pb content and moderate Cd level suitability of pelagic *Sargassum* as a starting material for processes aimed at producing food-grade alginate. Given that the extraction-purification procedure includes acid washing, ethanol precipitation, and pH-controlled precipitation/reconversion, residual inorganic contaminants in the resulting alginate are expected to be substantially reduced, consistent with food-grade specifications.

3.2. Optimization and yield of sodium alginate extracted from pelagic Sargassum

In brown seaweeds such as *Sargassum* spp., alginate occurs naturally as insoluble calcium and magnesium salts; efficient extraction therefore requires conversion of these forms into soluble sodium alginate through alkali-mediated cation exchange (FAO, 2003).

Fifteen experimental runs were conducted using the RSM-BBD to model the extraction of crude sodium alginate from pelagic *Sargassum* spp., with temperature (40-80 °C), extraction time (1-5 h), and Na_2CO_3 concentration (0.1-0.3 M) as independent variables. Crude sodium alginate yield varied between 16% and 41%, depending on the extraction conditions (Table 2). Using the composite desirability function developed by Derringer and Suich (1980), the optimal conditions were 80 °C, 5 h, and 0.3 M Na_2CO_3, with a desirability index of 1. Because the predicted optimum occurred at the upper bounds of all three factors, it represents a boundary optimum within the tested experimental domain.

The fitted second-order polynomial model describing crude yield as a function of temperature (A), time (B), and alkali concentration (C) was shown in Eq. (7). The model was highly significant ($F = 170$, $P < 0.0001$), with excellent fit statistics ($R^2 = 0.9922$, adjusted $R^2 = 0.9864$, predicted $R^2 = 0.9700$). Lack-of-fit was not significant ($F = 3.0$, $P = 0.276$), confirming model adequacy. All three linear terms (temperature,

time, and Na_2CO_3 concentration) were highly significant ($P < 0.0001$), along with the quadratic effects of A^2 ($P = 0.009$) and B^2 ($P < 0.0001$), and the A × B interaction term ($P = 0.010$) (Table 3).

$$\textit{Crude yield}\ (\%) = 5.38 - 0.272 \times \textit{Temp} + 7.148 \times \textit{Time} + 38.26 \times \textit{Alkali conc.} + 0.00404 \times \textit{Temp} \times \textit{Temp} - 1.062 \times \textit{Time} \times \textit{Time} + 0.0381 \times \textit{Temp} \times \textit{Time} \quad \text{Eq. 7}$$

It is important to note that the yields reported in the RSM-BBD analysis refer to crude sodium alginate recovery, calculated immediately after alkaline extraction and before bleaching and purification. The model predicted a maximum crude yield of 45.4%, and a confirmatory experiment under optimal conditions yielded 44.2%, validating the model's predictive capability. The factor ranges were intentionally constrained to remain operationally realistic and reproducible for scalable processing, avoiding unnecessarily harsh conditions that may increase energy demand and elevate the risk of polysaccharide degradation.

The effect of extraction time on crude yield was strongly influenced by temperature and alkali concentration. At 60 °C and 0.2 M Na_2CO_3, the yield increased from 20% at 1 h to 32% at 4 h, then plateaued. Under optimized temperature and extraction time, the yield increased steadily from 30% at 1 h to 45% at 5 h, demonstrating a 51% relative increase. This trend highlights the synergistic effect of temperature and time in enhancing extraction efficiency, likely due to improved matrix swelling, solubilization of alginate-calcium complexes, and increased mass transfer (Fig. 1a–b). Similar trends have been reported for other brown seaweeds, where yields rise with time and temperature but eventually plateau due to polymer degradation or saturation of extractable sodium alginate (Fawzy et al., 2017; Fenoradosoa et al., 2010; Mohammed et al., 2020).

The interaction between temperature and alkali concentration also influenced extraction outcomes. At 3 h, increasing Na_2CO_3 from 0.1 M to 0.3 M improved yield from 21% to 29% at 40 °C and from 34% to 42% at 80 °C. These data indicate that higher temperatures amplify the solubilizing effect of alkali, possibly by enhancing the dissociation of guluronic acid-Ca^{2+} cross-links and increasing alginate mobility in the aqueous phase (Mazumder et al., 2016) (Fig. 1c–d).

A similar interaction was observed between alkali concentration and extraction time at a fixed temperature (60 °C). At 1 h, increasing Na_2CO_3 from 0.1 M to 0.3 M increased yield from 16% to 24%, while at 5 h, the same increase raised yield from 28% to 36%. When holding Na_2CO_3 constant at 0.3 M, extending the extraction time from 1 h to 5 h improved the yield from 26% to 36%, representing a 10% absolute gain (Fig. 1e–f). These findings suggest that longer exposure to stronger alkaline conditions facilitates deeper diffusion into algal tissues and more effective solubilization of bound alginate (Bojorges, López-Rubio et al., 2023).

Taken together, these results confirm that temperature, time, and Na_2CO_3 concentration exert strong individual and interactive effects on sodium alginate extraction yield. The optimized parameters greatly enhanced recovery efficiency. Importantly, these conditions are aligned with industrial hydrocolloid processing standards, supporting the scalability of this extraction strategy. In this study, RSM optimization was performed using crude yield as the response to establish a high-yield baseline for pelagic *Sargassum* valorization; future work could implement multi-response optimization, such as yield together with viscosity/Mv and functional performance, to balance recovery with polymer integrity and end-use properties.

In contrast to the crude extraction yields, the values reported for the different pretreatment strategies represent purified sodium alginate obtained after acid precipitation, ethanol washing, and neutralization. Under the optimized extraction conditions, purified sodium alginate yield ranged from 16.3% to 21.6% across pretreatments (Fig. 2a). The untreated control yielded 20%, while autoclaving for 10 min and 30 min produced slightly lower yields of 18.5% and 16.3%, respectively. HPP pretreatments at 400 MPa and 600 MPa yielded 19.5% and 19.2%, respectively. Sonication for 10 min and 30 min produced the highest recoveries, 21.6% and 20.7%, although these differences were not statistically significant ($P \geq 0.05$) compared with the control.

Overall, the yields remained within a narrow range (16-22%), indicating that neither thermal nor non-thermal pretreatments markedly improved or impaired extractability. These results are consistent with the RSM-BBD trends, suggesting that the physical pretreatments applied here did not substantially influence alginate solubilization efficiency, whereas prolonged autoclaving caused a modest decline in recovery.

Table 3
ANOVA summary for the response surface model on crude sodium alginate yield.

	Coefficient estimate	Sum of squares	Degree of freedom	Mean square	F-value	*P*-value
Model	5.38	848.01	6	141.33	170.07	<0.001
Temp	−0.272	341.00	1	341.00	410.32	<0.001
Time	7.148	299.88	1	299.88	360.84	<0.001
Alkali Conc.	38.26	117.12	1	117.12	140.93	<0.001
Temp × Temp	0.00404	9.70	1	9.70	11.67	0.009
Time × Time	−1.062	66.99	1	66.99	80.60	<0.001
Temp × Time	0.0381	9.27	1	9.27	11.16	0.010
Error		6.65	8	0.83		
Lack-of-Fit		5.97	6	1.00	2.93	0.276
Pure Error		0.68	2	0.34		
Total		854.65	14			

3.3. Characterization of purified sodium alginate

3.3.1. FTIR characterization of sodium alginate

All alginate samples exhibited the characteristic FTIR spectra of sodium alginate, indicating the presence of key functional groups (Fig. 3). The asymmetric and symmetric stretching vibrations of carboxylate groups (COO^-) were observed at approximately 1600 cm^{-1} and 1400 cm^{-1}, respectively. Additional bands corresponding to saccharide ring structures were detected at 1080 cm^{-1} (C-C) and 1030 cm^{-1} (C-O), along with a broad envelope spanning 1200-900 cm^{-1}, attributed to C-O-C linkages and polysaccharide backbone vibrations. A weak band near 900 cm^{-1}, typically associated with guluronic acid residues, was consistently observed across all samples (Leal et al., 2008).

Band intensities varied between pretreatments without a consistent trend (Table S3), potentially due to minor differences in ATR contact, local hydration state, or partial chain scission (Jensen et al., 2015). However, no new absorption bands appeared in the 1800-800 cm^{-1} region, and the positions of major peaks remained stable (±2-3 cm^{-1}), indicating that functional group-level chemistry was unchanged.

These findings support the hypothesis that pretreatments primarily induced physical modifications, such as chain fragmentation or conformational changes, rather than chemical alterations to functional groups. This aligns with the expected non-oxidative, non-reactive nature of the applied pretreatments. Consequently, the observed differences in functional performance are more likely driven by changes in molecular size, chain flexibility, or entanglement, rather than alterations in backbone composition, as further supported by the similar M/G ratios determined from the ^1H NMR analysis.

3.3.2. Effect of pretreatments on the M/G ratio of sodium alginate

^1H NMR spectra of all sodium alginate samples displayed the expected anomeric proton signals corresponding to guluronic and

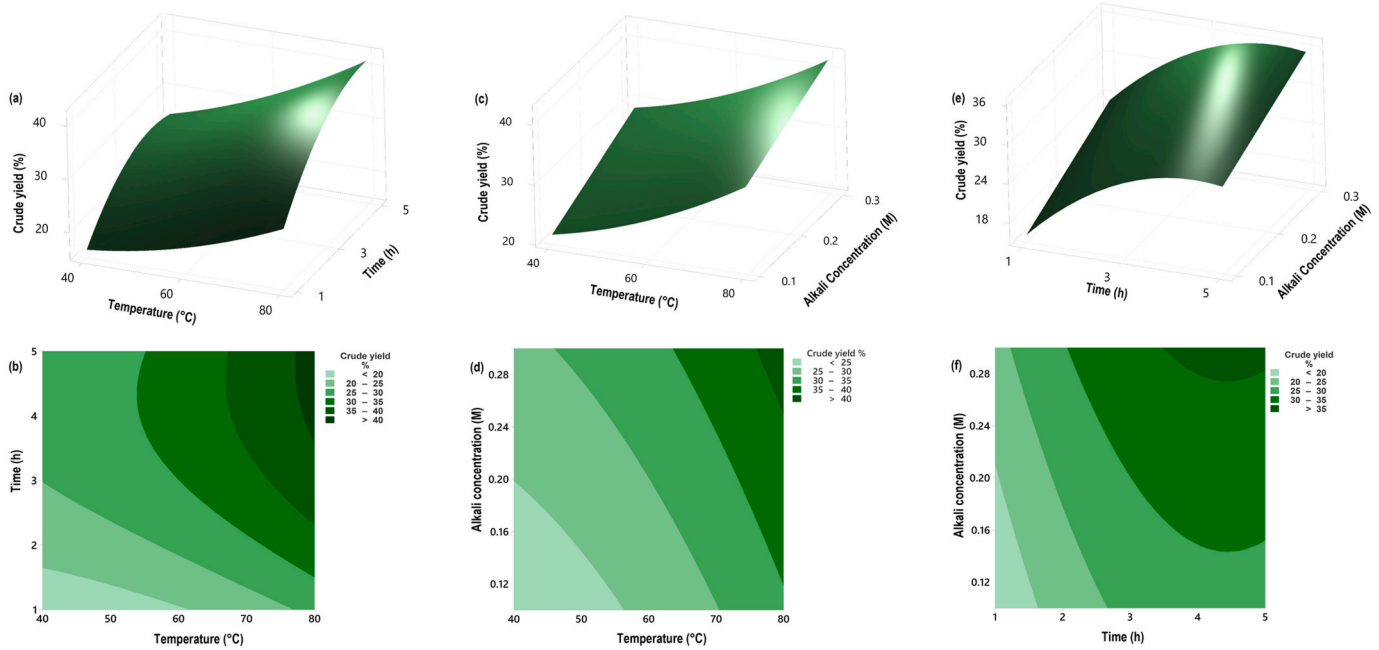

Fig. 1. Response surface analysis of crude yield of sodium alginate as a function of extraction parameters.
Three-dimensional response surface plots (a, c, and e) and corresponding two-dimensional contour plots (b, d, and f) show the interactive effects of three extraction parameters (temperature, time, and alkali concentration) on the crude yield (%) of alginate extracted from pelagic *Sargassum* spp. Panels (a) and (b) display the interaction between temperature (°C) and extraction time (h) at a fixed alkali concentration of 0.2 M. Panels (c) and (d) illustrate the effect of temperature (°C) and alkali concentration (M) at a fixed extraction time of 3 h. Panels (e) and (f) represent the interaction between extraction time (h) and alkali concentration (M) at a fixed temperature of 60 °C. In all experiments, the seaweed sample weight was 0.5 g, and the sample-to-alkali ratio was maintained at 1:50 (w/v).

mannuronic acid residues, confirming structural identity (Fig. 4). Three strong signals were observed at 5.56 ppm (G-1), 5.17 ppm (MM-1), and 4.96 ppm (GG-5). Additionally, three weaker resonances appeared on the low-field side of peak II at 5.25 ppm (GGM-5), 5.22 ppm (MGM-5), and 5.20 ppm (MG-1), corresponding to mixed-linkage protons commonly reported for brown algal alginates (Grasdalen, 1983; Grasdalen et al., 1979; Jensen et al., 2015; Kinh et al., 2014). While the resonance pattern and relative positions align well with published alginate spectra, the absolute chemical-shift values appear slightly downfield. Such variations are expected and likely arise from normal differences in solvent referencing, ionic environment, and experimental conditions inherent to NMR analysis of polysaccharides (Yao et al., 2021).

Quantitative integration of the anomeric region enabled estimation of monomer fractions (F_G, F_M) and M/G ratio (Table 4). The complete set of equations and calculations is provided in the Supplementary Material. All samples exhibited a guluronic acid-rich composition, with F_G values ranging from 0.74 to 0.80 and M/G ratios ranging from 0.25 to 0.35. No statistically significant differences were observed between pretreatments ($P \geq 0.05$), suggesting that pretreatments did not alter the monomer composition or blockwise sequence distribution.

Although M/G ratios were significantly similar, subtle variations may still influence functionality. For example, the slightly lower M/G values observed in sonicated samples may synergize with their higher M_v to enhance gel strength. Conversely, samples with marginally higher M/G ratios but lower M_v (e.g., autoclaved or HPP-600) may form weaker gels due to insufficient chain length, highlighting the interplay between composition and chain architecture (Yang et al., 2022).

Overall, these NMR results support the notion that functional differences observed among pretreatments primarily stem from changes in molecular structure (e.g., chain length, flexibility, or conformation) rather than from shifts in chemical composition or sequence.

3.4. Effect of pretreatments on the physicochemical and functional properties of purified sodium alginate

Pretreatments markedly altered both the molecular integrity and functional performance of the extracted sodium alginate. Key properties affected included apparent and intrinsic viscosity, M_v, gel strength, and E_{24}, each reflecting distinct structural changes induced by thermal and non-thermal processing (Fig. 2b–f).

The untreated control exhibited the highest intrinsic viscosity (2.90 dL/g) and M_v (136 kDa), reflecting an intact, high-M_v polymer network (Ravve, 2012). Its apparent viscosity was also high (14.1 mPa s), consistent with limited chain fragmentation and extensive molecular entanglement typical of minimally processed alginate.

Autoclaving produced the most severe degradation among all pretreatments, reducing apparent viscosity (3.23 mPa s), intrinsic viscosity (0.32 dL/g), and M_v (14.6 kDa) to a fraction of the control values. Gel strength likewise declined from 175 g to 77 g. This overall decrease in viscosity, M_v, and gel strength indicates the severe depolymerization and conformational disruption caused by prolonged thermal exposure (Chansoria et al., 2020), likely attributed to acid hydrolysis or heat-induced glycosidic bond cleavage (Lorson et al., 2020).

Sonication exerted a time-dependent but comparatively mild impact on alginate structure. After 10 min, M_v remained relatively high (83 kDa), and gel strength (144-174 g) was largely preserved, indicating limited backbone cleavage under low-intensity ultrasound (Feng et al., 2017). Extending treatment to 30 min induced minor reductions in M_v (77 kDa) and viscosity, suggesting controlled fragmentation rather than extensive degradation (Wu et al., 2025).

In contrast to viscosity and gel behavior, emulsification performance diverged sharply among pretreatments. Despite their relatively high M_v, sonicated samples exhibited low E_{24} values (4.69–7.81%), suggesting that semi-rigid, entangled chains diffuse slowly to the oil–water interface and form less effective interfacial films (Wardhani et al., 2021). It should be noted that sodium alginate is predominantly hydrophilic and has limited intrinsic amphiphilicity, which can constrain its ability to

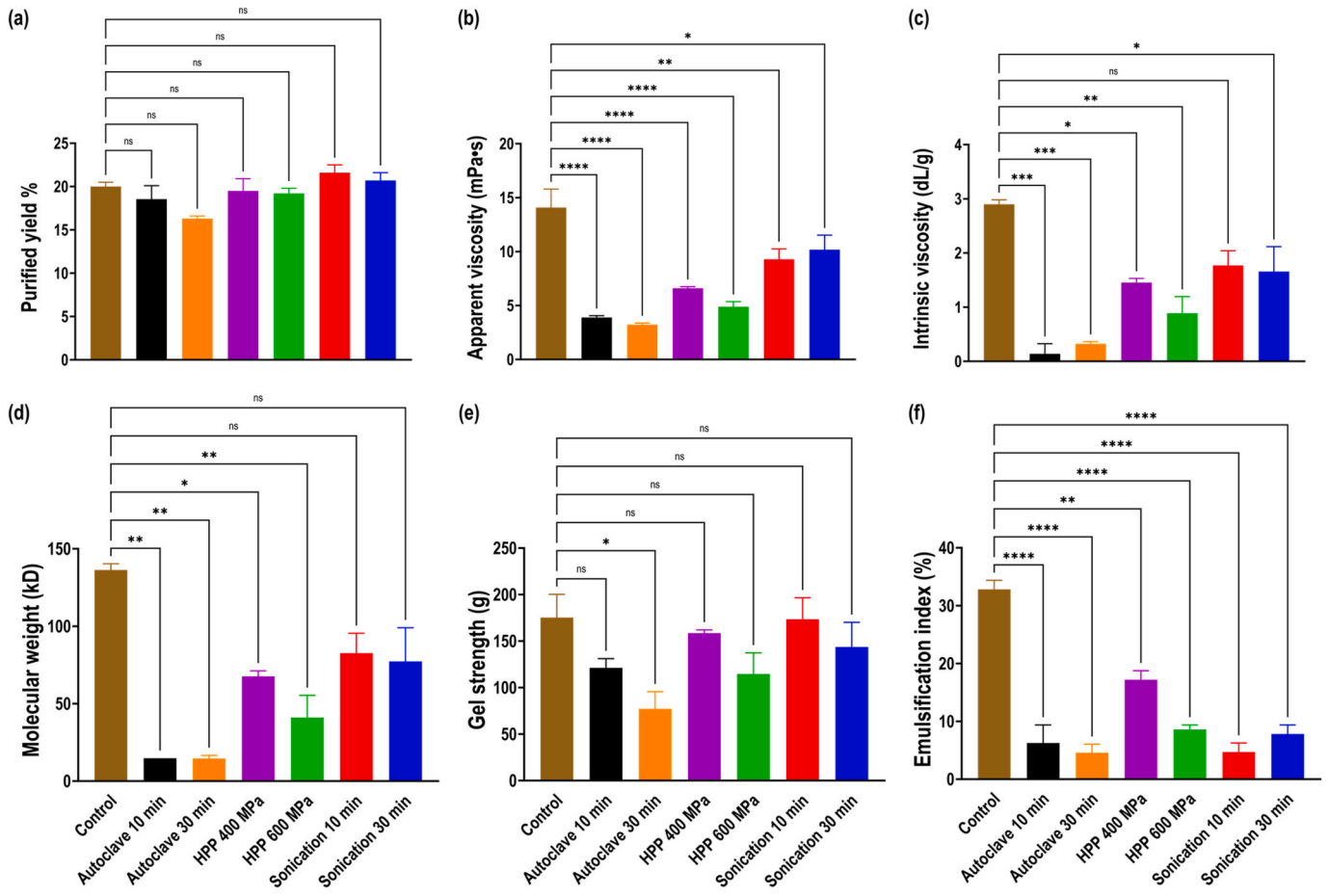

Fig. 2. Effect of different pretreatments on the physicochemical and functional properties of sodium alginate purified from pelagic *Sargassum* spp. The comparison includes a control (no pretreatment) along with six pretreatment conditions: autoclaving at 121 °C and 35 psi for 10 and 30 min, HPP at 400 and 600 MPa for 10 min at RT, and sonication at 40 kHz for 10 and 30 min at RT. Bars represent mean ± SEM (n = 2).
Significant levels: $P \geq 0.05$ (not significant (ns)), $P = 0.0332$ (*), $P = 0.0021$ (**), $P = 0.0002$ (***), $P < 0.0001$ (****).

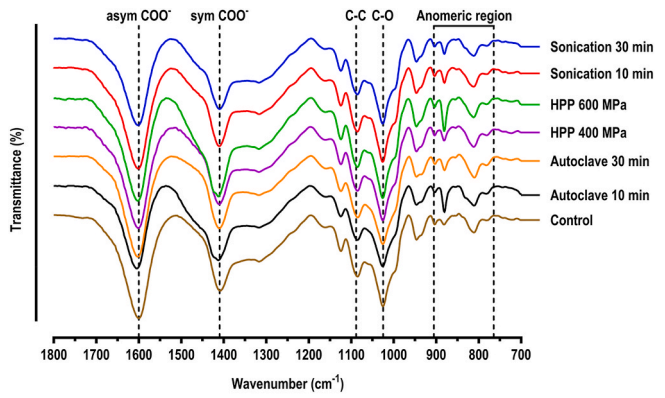

Fig. 3. FTIR spectra of sodium alginate purified from pelagic *Sargassum* spp. under control and pretreatment conditions.
The spectra represent the control (no pretreatment) along with six pretreatment conditions: autoclaving at 121 °C and 35 psi for 10 and 30 min, HPP at 400 and 600 MPa for 10 min at RT, and sonication at 40 kHz for 10 and 30 min at RT. Spectra were recorded in the range of 1800-700 cm^{-1} to highlight key functional group vibrations.

rapidly adsorb and lower interfacial tension compared with true surface-active emulsifiers (Akshaya & Nathanael, 2024). In many food emulsion systems, alginate therefore contributes to stability mainly through continuous-phase thickening and/or by forming interfacial structures via complexation or gel-like shells/particles at the oil-water interface, rather than by acting as a primary emulsifier (Gao et al., 2023). From this perspective, higher molecular weight and stronger chain entanglement (as reflected by higher intrinsic/apparent viscosity) may favor gel strength, yet can also slow interfacial transport and rearrangement, leading to weaker short-term emulsification indices when adsorption/coverage is rate-limiting (Charisis & Kalogianni, 2023).

HPP at 400 MPa produced the highest E_{24} (17.2%), coinciding with a moderate M_v (67.6 kDa) and reduced intrinsic viscosity. A plausible explanation is that partial reduction in chain length and entanglement increases polymer mobility, enabling faster redistribution during emulsification and improved droplet stabilization. In alginate-based systems, stabilization can arise from interfacial structuring (Charisis & Kalogianni, 2023) and/or electrostatic deposition onto oppositely charged, protein-coated droplets (Ma et al., 2017). Although interfacial tension, droplet size, and ζ-potential were not measured, these mechanisms support why moderate molecular weight/viscosity alginate may stabilize emulsions more effectively than highly entangled, high molecular weight alginate. Similar findings have been reported in high-pressure-treated (X. Zhang et al., 2023) and structurally modified alginates (Bojorges, Martínez-Abad, et al., 2023).

Collectively, these results demonstrate that thermal degradation significantly impairs both molecular integrity and functionality, while non-thermal pretreatments, particularly sonication and HPP at 400 MPa, better preserve alginate performance. However, no direct one-to-one correspondence was observed between M_v, viscosity, gel strength,

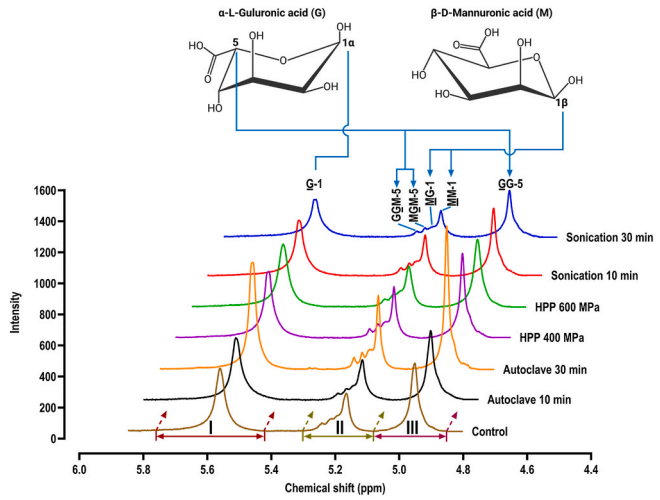

Fig. 4. ^{1}H NMR spectra of sodium alginate purified from pelagic *Sargassum* spp. under control and pretreatment conditions in D_2O at 80 °C The spectra represent the control (no pretreatment) along with six pretreatment conditions: autoclaving at 121 °C and 35 psi for 10 and 30 min, HPP at 400 and 600 MPa for 10 min at RT, and sonication at 40 kHz for 10 and 30 min at RT. NMR spectra highlight the characteristic proton resonances of α-L-guluronic acid (G) and β-D-mannuronic acid (M) residues. Major chemical shifts include: Peak I (5.76-5.42 ppm, maroon dashed arrows): H-1 of G (G-1); Peak II (5.30-5.08 ppm, olive green dashed arrows): Overlapping signals from H-1 of M (MM-1), and mixed blocks (GGM-5, MGM-5, MG-1); Peak III (5.08-4.85 ppm, deep magenta dashed arrows): H-5 of G (GG-5) in G-G diads. The underlined letters (e.g., MG-1, GGM-5) indicate the residue from which the observed proton originates. The structures of G and M are shown to demonstrate the proton environments corresponding to each signal. Three peaks (I, II, and III) denote the three major regions used for integration-based estimation of M/G ratios. Variations in peak intensities and relative distributions reflect compositional and sequence differences in alginate due to different pretreatments. (For interpretation of the references to colour in this figure legend, the reader is referred to the Web version of this article.)

and E_{24}, reflecting the complex and multifactorial nature of alginate structure-function relationships.

Although the control exhibited the highest M_v and gel strength, it lacked the tailored functionalities observed in treated samples. Thus, the practical value of pretreatment is not to outperform the control universally, but to provide a controllable processing lever to tailor alginate performance to the intended end use. Non-thermal methods, in particular, allowed selective enhancement of emulsification (HPP) or preservation of gel strength (sonication), highlighting their value for application-specific design of food hydrocolloids.

Overall, a clear pattern emerged: high M_v correlated with strong gels and high viscosity, while moderate M_v (60-70 kDa) appeared optimal for emulsification. Among all pretreatments, autoclaving was the least favorable, severely compromising alginate performance. In contrast, mild sonication and moderate HPP preserved or selectively enhanced specific functionalities.

These findings suggest that non-thermal pretreatments offer promising tools for tuning alginate properties for application-specific performance. HPP may be preferable for formulations requiring enhanced emulsifying capacity, such as salad dressings or beverages, whereas sonication may be better suited for applications requiring strong gels, such as dessert matrices or encapsulation systems.

4. Conclusion

This study demonstrates that pretreatment strategies significantly influence the structural and functional properties of sodium alginate extracted from pelagic *Sargassum* spp., offering a value-added route for utilizing this underused biomass. Autoclaving caused severe depolymerization, resulting in reduced M_v, viscosity, gel strength, and emulsification capacity, rendering it unsuitable for food applications. In contrast, non-thermal pretreatments, specifically sonication (10 min) and high-pressure processing (400 MPa), selectively enhanced desirable functional attributes.

Sonication preserved molecular integrity and maximized gel strength, supporting its use in gels, encapsulates, and structured hydrocolloid systems. HPP improved the E_{24}, indicating potential for emulsion-based food products such as dressings and beverages. FTIR and NMR analyses confirmed that the alginate backbone remained chemically stable, suggesting that functional changes were driven by controlled chain disentanglement, flexibility, or conformational changes rather than chemical modification.

Overall, this study demonstrates that non-thermal pretreatments can modulate alginate functionality without altering chemical integrity, providing opportunities to tailor alginate properties for specific clean-label food applications. While these methods did not outperform the control, their selective effects demonstrate feasible pathways for application-specific optimization. Importantly, by enabling the production of functional alginate from pelagic *Sargassum* with potential for food-related applications, this work offers an alternative, sustainable strategy to valorize this abundant marine biomass. A logical next step toward commercialization is batch-to-batch verification of regulated metals/metalloids in the purified alginate, alongside functional testing in model food systems. Future work should focus on optimizing these pretreatment conditions and evaluating their performance in model food systems to better align alginate functionality with targeted product needs.

CRediT authorship contribution statement

Aravind Kumar Bingi: Writing – review & editing, Writing –

Table 4
Monosaccharide composition (F_G, F_{GG}, F_M) and M/G ratio of sodium alginate purified from pelagic *Sargassum* spp. under control and pretreatment conditions.

Samples		F_G	F_{GG}	F_M	M/G
Control		0.76 ± 0.02[a]	0.58 ± 0.01	0.24 ± 0.02	0.31 ± 0.03
Pretreatments					
Autoclave	10 min	0.74 ± 0.01[a]	0.59 ± 0.01[a]	0.26 ± 0.01[a]	0.35 ± 0.01[a]
	30 min	0.75 ± 0.01[a]	0.61 ± 0.00[b]	0.25 ± 0.01[a]	0.34 ± 0.02[a]
HPP	400 MPa	0.76 ± 0.01[a]	0.59 ± 0.00[a]	0.24 ± 0.01[a]	0.32 ± 0.01[a]
	600 MPa	0.76 ± 0.02[a]	0.59 ± 0.00[a]	0.24 ± 0.02[a]	0.32 ± 0.03[a]
Sonication	10 min	0.78 ± 0.03[a]	0.58 ± 0.00[a]	0.23 ± 0.03[a]	0.29 ± 0.05[a]
	30 min	0.80 ± 0.00[a]	0.58 ± 0.00[a]	0.20 ± 0.00[a]	0.25 ± 0.00[a]

F_G: Fraction of guluronic acid.
F_{GG}: Fraction of guluronic acid-guluronic acid dimer.
F_M: Fraction of mannuronic acid.
[a,b] Means with different superscripts differ significantly from the control ($P < 0.05$).
[a] Values are presented as mean ± SEM.

original draft, Validation, Methodology, Investigation, Formal analysis, Data curation. **Yaqi Zhao:** Writing – review & editing, Methodology, Investigation. **Yu-Jou Chou:** Writing – review & editing, Investigation. **Chunya Tang:** Methodology, Investigation. **Banghao Chen:** Methodology, Investigation. **Jeremy D. Owens:** Methodology, Investigation. **Brian E. Lapointe:** Investigation. **Rachel A. Brewton:** Investigation. **Imran Ahmad:** Investigation. **Qinchun Rao:** Writing – review & editing, Supervision, Resources, Project administration, Methodology, Funding acquisition, Conceptualization.

Declaration of competing interest

The authors declare that they have no known competing financial interests or personal relationships that could have appeared to influence the work reported in this paper.

Acknowledgments

This work was supported by the National Institute of Food and Agriculture, US Department of Agriculture (2020-67017-33236, 202270001-37580, and 2023-38821-39580).

Appendix A. Supplementary data

Supplementary data to this article can be found online at https://doi.org/10.1016/j.foodhyd.2026.112534.

Data availability

Data will be made available on request.

References

Akshaya, S., & Nathanael, A. J. (2024). A review on hydrophobically associated alginates: Approaches and applications. *ACS Omega, 9*(4), 4246–4262. https://doi.org/10.1021/acsomega.3c08619

Andreou, V., Dimopoulos, G., Alexandrakis, Z., Katsaros, G., Oikonomou, D., Toepfl, S., Heinz, V., & Taoukis, P. (2017). Shelf-life evaluation of virgin olive oil extracted from olives subjected to nonthermal pretreatments for yield increase. *Innovative Food Science & Emerging Technologies, 40*, 52–57. https://doi.org/10.1016/j.ifset.2016.09.009

ASTM-F2259-10. (2012). Standard test method for determining the chemical composition and sequence in alginate by proton nuclear magnetic resonance (^{1}H NMR) spectroscopy. https://compass.astm.org/content-access?contentCode=ASTM%7CF2259-10%7Cen-US.

Balboa, E. M., Moure, A., & Domínguez, H. (2015). Valorization of *Sargassum muticum* biomass according to the biorefinery concept. *Marine Drugs, 13*(6), 3745–3760. https://doi.org/10.3390/md13063745

Bauta, J., Calbrix, E., Capblancq, S., Cecutti, C., Peydecastaing, J., Raynaud, C. D., Rouilly, A., Simon, V., Vaca-Medina, G., & Vandenbossche, V. (2024). Global chemical characterization of *Sargassum* spp. Seaweeds from different locations on Caribbean islands: A screening of organic compounds and heavy metals contents. *Phycology, 4*(2), 190–212. https://doi.org/10.3390/phycology4020011

Bojorges, H., López-Rubio, A., Martínez-Abad, A., & Fabra, M. J. (2023). Overview of alginate extraction processes: Impact on alginate molecular structure and techno-functional properties. *Trends in Food Science & Technology, 140*, Article 104142. https://doi.org/10.1016/j.tifs.2023.104142

Bojorges, H., Martínez-Abad, A., Martínez-Sanz, M., Rodrigo, M. D., Vilaplana, F., López-Rubio, A., & Fabra, M. J. (2023). Structural and functional properties of alginate obtained by means of high hydrostatic pressure-assisted extraction. *Carbohydrate Polymers, 299*, Article 120175. https://doi.org/10.1016/j.carbpol.2022.120175

Canul-Ku, L. A., Sanginés-García, J. R., Urquizo, E. A., Canul-Solís, J. R., Valdivieso-Pérez, I. A., Vargas-Bello-Pérez, E., Molina-Botero, I., Arango, J., & Piñeiro-Vázquez, Á. T. (2023). Effect of pelagic *Sargassum* on in vitro dry matter and organic matter degradation, gas production, and protozoa population. *Animals, 13*(11), 1858. https://doi.org/10.3390/ani13111858

Carrillo-Domínguez, S., Rodríguez-Martínez, R. E., Díaz-Martínez, M., Magaña-Gallegos, E., & Cuchillo-Hilario, M. (2023). Potential application of pelagic *Sargassum* spp. in animal feeding. *Journal of Applied Phycology, 35*(1), 433–444. https://doi.org/10.1007/s10811-022-02877-x

Chansoria, P., Narayanan, L. K., Wood, M., Alvarado, C., Lin, A., & Shirwaiker, R. A. (2020). Effects of autoclaving, EtOH, and UV sterilization on the chemical, mechanical, printability, and biocompatibility characteristics of alginate. *ACS Biomaterials Science & Engineering, 6*(9), 5191–5201. https://doi.org/10.1021/acsbiomaterials.0c00806?ref=pdf

Charisis, A., & Kalogianni, E. P. (2023). Alginate-chitosan microgel particles, water–oil interfacial layers, and emulsion stabilization. *Colloids and Interfaces, 7*, 48.

Chee, S.-Y., Wong, P.-K., & Wong, C.-L. (2011). Extraction and characterisation of alginate from brown seaweeds (Fucales, Phaeophyceae) collected from Port Dickson, Peninsular Malaysia. *Journal of Applied Phycology, 23*(2), 191–196. https://doi.org/10.1007/s10811-010-9533-7

Cherry, P., O'Hara, C., Magee, P. J., McSorley, E. M., & Allsopp, P. J. (2019). Risks and benefits of consuming edible seaweeds. *Nutrition Reviews, 77*(5), 307–329. https://doi.org/10.1093/nutrit/nuy066

Chikani-Cabrera, K. D., Fernandes, P. M. B., Tapia-Tussell, R., Parra-Ortiz, D. L., Hernández-Zárate, G., Valdez-Ojeda, R., & Alzate-Gaviria, L. (2022). Improvement in methane production from pelagic *Sargassum* using combined pretreatments. *Life, 12*(8), 1214. https://doi.org/10.3390/life12081214

Codex Alimentarius Commission. (2024). General standard for contaminants and toxins in food and feed. https://www.fao.org/fao-who-codexalimentarius/sh-proxy/fr/?lnk=1&url=https%253A%252F%252Fworkspace.fao.org%252Fsites%252Fcodex%252FStandards%252FCXS%2B193-1995%252FCXS_193e.pdf.

Contreras, L., Ritter, A., Dennett, G., Boehmwald, F., Guitton, N., Pineau, C., Moenne, A., Potin, P., & Correa, J. A. (2008). Two-dimensional gel electrophoresis analysis of brown algal protein extracts. *Journal of Phycology, 44*(5), 1315–1321. https://doi.org/10.1111/j.1529-8817.2008.00575.x

Derringer, G., & Suich, R. (1980). Simultaneous optimization of several response variables. *Journal of Quality Technology, 12*(4), 214–219. https://doi.org/10.1080/00224065.1980.11980968

Díaz-Vázquez, L. M., Rojas-Pérez, A., Fuentes-Caraballo, M., Robles, I. V., Jena, U., & Das, K. C. (2015). Demineralization of *Sargassum* spp. macroalgae biomass: Selective hydrothermal liquefaction process for bio-oil production. *Frontiers in Energy Research, 3*. https://doi.org/10.3389/fenrg.2015.00006, 2015.

Din, S. S., Chew, K. W., Chang, Y.-K., Show, P. L., Phang, S. M., & Juan, J. C. (2019). Extraction of agar from *Eucheuma cottonii* and *Gelidium amansii* seaweeds with sonication pretreatment using autoclaving method. *Journal of Oceanology and Limnology, 37*(3), 871–880. https://doi.org/10.1007/s00343-019-8145-6

Djemaa, I. B., Boulmedais, F., Auguste, S., Tarnowska, M., Andrieux, S., & Drenckhan-Andreatta, W. (2024). Glucono-delta-lactone-induced alginate gelation: New insights into the effect of the cross-linker carrier type on the hydrogel mechanics. *Langmuir, 40*(20), 10492–10501. https://doi.org/10.1021/acs.langmuir.3c03959

FAO. (2003). A guide to the seaweed industry. *FAO Fisheries Technical Paper, 441*, 105. https://www.fao.org/4/y4765e/y4765e00.htm.

Fawzy, M. A., Gomaa, M., Hifney, A. F., & Abdel-Gawad, K. M. (2017). Optimization of alginate alkaline extraction technology from *Sargassum latifolium* and its potential antioxidant and emulsifying properties. *Carbohydrate Polymers, 157*, 1903–1912. https://doi.org/10.1016/j.carbpol.2016.11.077

FDA. (2018a). *Guidance for industry: Juice hazard analysis critical control point hazards and controls guidance* (1st ed.) Retrieved from https://www.fda.gov/regulatory-information/search-fda-guidance-documents/guidance-industry-juice-hazard-analysis-critical-control-point-hazards-and-controls-guidance-first. (Accessed 28 November 2025).

FDA. (2018b). Guidance for industry: Lead in candy likely to be consumed frequently by small children. Retrieved from https://www.fda.gov/regulatory-information/search-fda-guidance-documents/guidance-industry-lead-candy-likely-be-consumed-frequently-small-children#ftn2. (Accessed 28 November 2025).

FDA. (2024). Cadmium in food and foodwares. Retrieved from https://www.fda.gov/food/environmental-contaminants-food/cadmium-food-and-foodwares. (Accessed 28 November 2025).

Feng, L., Cao, Y., Xu, D., Wang, S., & Zhang, J. (2017). Molecular weight distribution, rheological property and structural changes of sodium alginate induced by ultrasound. *Ultrasonics Sonochemistry, 34*, 609–615. https://doi.org/10.1016/j.ultsonch.2016.06.038

Fenoradosoa, T. A., Ali, G., Delattre, C., Laroche, C., Petit, E., Wadouachi, A., & Michaud, P. (2010). Extraction and characterization of an alginate from the brown seaweed *Sargassum turbinarioides* Grunow. *Journal of Applied Phycology, 22*(2), 131–137. https://doi.org/10.1007/s10811-009-9432-y

Gao, Z., Gao, C., J, W., Xu, L., Hu, B., Yao, X., Li, Y., & Wu, Y. (2023). In situ crosslinking sodium alginate on oil-water interface to stabilize the O/W emulsions. *Food Hydrocolloids, 135*, Article 108233. https://doi.org/10.1016/j.foodhyd.2022.108233

Gower, J., Young, E., & King, S. (2013). Satellite images suggest a new *Sargassum* source region in 2011. *Remote Sensing Letters, 4*(8), 764–773. https://doi.org/10.1080/2150704X.2013.796433

GraphPad. (2025). Outlier calculator. Retrieved from https://www.graphpad.com/quickcalcs/grubbs1/. (Accessed 28 November 2025).

Grasdalen, H. (1983). High-field, ^{1}H-N.M.R. spectroscopy of alginate: Sequential structure and linkage conformations. *Carbohydrate Research, 118*, 255–260. https://doi.org/10.1016/0008-6215(83)88053-7

Grasdalen, H., Larsen, B., & Smidsrød, O. (1979). A p.m.r. study of the composition and sequence of uronate residues in alginates. *Carbohydrate Research, 68*(1), 23–31. https://doi.org/10.1016/S0008-6215(00)84051-3

Hernández-Carmona, G., McHugh, D. J., & López-Gutiérrez, F. (1999). Pilot plant scale extraction of alginates from *Macrocystis pyrifera*. 2. Studies on extraction conditions and methods of separating the alkaline-insoluble residue. *Journal of Applied Phycology, 11*(6), 493–502. https://doi.org/10.1023/A:1008114709681

Jensen, H. M., Larsen, F. H., & Engelsen, S. B. (2015). Characterization of alginates by nuclear magnetic resonance (NMR) and vibrational spectroscopy (IR, NIR, Raman) in combination with chemometrics. In D. B. Stengel, & S. Connan (Eds.), *Natural products From Marine algae: Methods and protocols* (pp. 347–363). New York, NY: Springer New York. https://doi.org/10.1007/978-1-4939-2684-8_22.

Jung, K. A., Lim, S.-R., Kim, Y., & Park, J. M. (2013). Potentials of macroalgae as feedstocks for biorefinery. *Bioresource Technology, 135*, 182–190. https://doi.org/10.1016/j.biortech.2012.10.025

Kinh, C. D., Thien, T. V., Hoa, T. T., & Khieu, D. Q. (2014). Interpretation of ^{1}H-NMR spectrum of alginate by ^{1}H-^{1}H TOCSY and COSY spectrum. *Vietnam Journal of Chemistry, 45*(6), 772. https://doi.org/10.15625/4829

Lapointe, B. E., Webber, D. F., & Brewton, R. A. (2025). Productivity, growth, and biogeochemistry of pelagic *Sargassum* in a changing world. *Harmful Algae, 150*, Article 102940. https://doi.org/10.1016/j.hal.2025.102940

Leal, D., Matsuhiro, B., Rossi, M., & Caruso, F. (2008). FT-IR spectra of alginic acid block fractions in three species of brown seaweeds. *Carbohydrate Research, 343*(2), 308–316. https://doi.org/10.1016/j.carres.2007.10.016

Leal-Bautista, R. M., Rodriguez-Garcia, J. C., Acosta-González, G., Chablé-Villacis, R., Tapia-Tussell, R., Bautista-García, J. E., Olguìn-Maciel, E., Alzate-Gaviria, L., & González-López, G. (2024). Assessment of leachate generated by *Sargassum* spp. in the Mexican caribe: Part 1 spatial variations. *Water, 16*(9), 1251. https://doi.org/10.3390/w16091251

Lee, J.-W., Choi, H., Hwang, U.-K., Kang, J.-C., Kang, Y. J., Kim, K. I., & Kim, J.-H. (2019). Toxic effects of lead exposure on bioaccumulation, oxidative stress, neurotoxicity, and immune responses in fish: A review. *Environmental Toxicology and Pharmacology, 68*, 101–108. https://doi.org/10.1016/j.etap.2019.03.010

Lee, M.-C., Yeh, H.-Y., Chang, C.-M., Liou, Y.-F., Nan, F.-H., & Wungen-Sani, J. (2023). Tracking and utilizing *Sargassum*, an abundant resource from the Caribbean Sea. *Water, 15*(15), 2694. https://doi.org/10.3390/w15152694

Liranzo-Gómez, R. E., Gómez, A. M., Gómez, B., González-Hernández, Y., & Jauregui-Haza, U. J. (2023). Characterization of *Sargassum* accumulated on Dominican beaches in 2021: Analysis of heavy, alkaline and alkaline-earth metals, proteins and fats. *Marine Pollution Bulletin, 193*, Article 115120. https://doi.org/10.1016/j.marpolbul.2023.115120

Lorson, T., Ruopp, M., Nadernezhad, A., Eiber, J., Vogel, U., Jungst, T., & Lühmann, T. (2020). Sterilization methods and their influence on physicochemical properties and bioprinting of alginate as a bioink component. *ACS Omega, 5*(12), 6481–6486. https://doi.org/10.1021/acsomega.9b04096

Ma, D., Tu, Z.-C., Wang, H., Zhang, Z., & McClements, D. J. (2017). Fabrication and characterization of nanoemulsion-coated microgels: Electrostatic deposition of lipid droplets on alginate beads. *Food Hydrocolloids, 71*, 149–157. https://doi.org/10.1016/j.foodhyd.2017.05.015

Makkar, H. P. S., Tran, G., Heuzé, V., Giger-Reverdin, S., Lessire, M., Lebas, F., & Ankers, P. (2016). Seaweeds for livestock diets: A review. *Animal Feed Science and Technology, 212*, 1–17. https://doi.org/10.1016/j.anifeedsci.2015.09.018

Mazumder, A., Holdt, S. L., De Francisci, D., Alvarado-Morales, M., Mishra, H. N., & Angelidaki, I. (2016). Extraction of alginate from *Sargassum muticum*: Process optimization and study of its functional activities. *Journal of Applied Phycology, 28*(6), 3625–3634. https://doi.org/10.1007/s10811-016-0872-x

McHugh, D. J., Hernández-Carmona, G., Arvizu-Higuera, D. L., & Rodríguez-Montesinos, Y. E. (2001). Pilot plant scale extraction of alginates from *Macrocystis pyrifera* 3. Precipitation, bleaching and conversion of calcium alginate to alginic acid. *Journal of Applied Phycology, 13*(6), 471–479. https://doi.org/10.1023/A:1012532706235

Melchor-Martínez, E. M., Reyes, A. G., Morreeuw, Z. P., Flores-Contreras, E. A., Araújo, R. G., Ramírez-Gamboa, D., Sosa-Hernández, J. E., Iqbal, H. M. N., González-Meza, G. M., Bonaccorso, A. D., Peña-Rodríguez, A., & Parra-Saldívar, R. (2023). Comparative study on the valorization of *Sargassum* from the Mexican Caribbean coast and Gulf of California as an ingredient on healthy diets for shrimp farming. *Aquaculture Reports, 32*, Article 101709. https://doi.org/10.1016/j.aqrep.2023.101709

Milledge, J. J., Maneein, S., Arribas López, E., & Bartlett, D. (2020). *Sargassum* inundations in Turks and Caicos: Methane potential and proximate, ultimate, lipid, amino acid, metal and metalloid analyses. *Energies, 13*(6), 1523. https://doi.org/10.3390/en13061523

Mohammed, A., Rivers, A., Stuckey, D. C., & Ward, K. (2020). Alginate extraction from *Sargassum* seaweed in the Caribbean region: Optimization using response surface methodology. *Carbohydrate Polymers, 245*, Article 116419. https://doi.org/10.1016/j.carbpol.2020.116419

Nielsen, B. V., Milledge, J. J., Hertler, H., Maneein, S., Al Farid, M. M., & Bartlett, D. (2021). Chemical characterisation of *Sargassum* inundation from the Turks and Caicos: Seasonal and post stranding changes. *Phycology, 1*(2), 11. https://doi.org/10.3390/phycology1020011

Olguin-Maciel, E., Leal-Bautista, R. M., Alzate-Gaviria, L., Domínguez-Maldonado, J., & Tapia-Tussell, R. (2022). Environmental impact of *Sargassum* spp. landings: An evaluation of leachate released from natural decomposition at Mexican Caribbean coast. *Environmental Science and Pollution Research, 29*(60), 91071–91080. https://doi.org/10.1007/s11356-022-22123-8

Pawar, S. N., & Edgar, K. J. (2012). Alginate derivatization: A review of chemistry, properties and applications. *Biomaterials, 33*(11), 3279–3305. https://doi.org/10.1016/j.biomaterials.2012.01.007

Pournaki, S. K., Aleman, R. S., Hasani-Azhdari, M., Marcia, J., Yadav, A., & Moncada, M. (2024). *Current review: Alginate in the food applications. J, 7*(3), 281–301. https://doi.org/10.3390/j7030016

Pragatheeswari, R., & Raajeswari, P. (2024). Property analysis of sodium alginate from brown macroalgae (*Sargassum cinctum* J.Agardh). *The Journal of Research ANGRAU, 52*, 85–93. https://doi.org/10.58537/jorangrau.2024.52.1.10

Purcell-Meyerink, D., Packer, M. A., Wheeler, T. T., & Hayes, M. (2021). Aquaculture production of the brown seaweeds *Laminaria digitata* and *Macrocystis pyrifera*: Applications in food and pharmaceuticals. *Molecules, 26*(5), 1306. https://doi.org/10.3390/molecules26051306

Ravve, A. (2012). *Principles of polymer chemistry*. New York: Springer. https://doi.org/10.1007/978-1-4614-2212-9

Rodríguez-Rodríguez, Y., Soldevilla-Hernández, L. I., Guevara, M.Á., Gandini, G., & Jáuregui-Haza, U. J. (2025). Assessment of a *Sargassum*-based liquid biofertilizer for enhanced banana cultivation in small-scale family farms. *Case Studies in Chemical and Environmental Engineering, 12*, Article 101252. https://doi.org/10.1016/j.cscee.2025.101252

Rostami, Z., Tabarsa, M., You, S., & Rezaei, M. (2017). Relationship between molecular weights and biological properties of alginates extracted under different methods from *Colpomenia peregrina*. *Process Biochemistry, 58*, 289–297. https://doi.org/10.1016/j.procbio.2017.04.037

Ruslan, R., Amir, A., & Wiraningtyas, A. (2019). Extraction of sodium alginate from *Sargassum sp*. using microwave-assisted extraction (MAE). *The Journal of Pure and Applied Chemistry Research, 8*, 23–30. https://doi.org/10.21776/ub.jpacr.2019.008.01.420

Salgado-Hernández, E., Alvarado-Lassman, A., Martínez-Hernández, S., Velázquez-Fernández, J. B., Dorantes-Acosta, A. E., Rosas-Mendoza, E. S., & Ortiz-Ceballos, Á. I. (2023). Energy-saving pretreatments affect pelagic *Sargassum* composition and DNA metabarcoding analysis reveals the microbial community involved in methane yield. *bioRxiv, 2023*, Article 533673. https://doi.org/10.1101/2023.03.21.533673, 2003.2021.

Salgado-Hernández, E., Ortiz-Ceballos, Á. I., Martínez-Hernández, S., Rosas-Mendoza, E. S., Dorantes-Acosta, A. E., Alvarado-Vallejo, A., & Alvarado-Lassman, A. (2023). Methane production of *Sargassum* spp. Biomass from the Mexican Caribbean: Solid–liquid separation and component distribution. *International Journal of Environmental Research and Public Health, 20*(1), 219. https://doi.org/10.3390/ijerph20010219

Saravana, P. S., Cho, Y.-N., Woo, H.-C., & Chun, B.-S. (2018). Green and efficient extraction of polysaccharides from brown seaweed by adding deep eutectic solvent in subcritical water hydrolysis. *Journal of Cleaner Production, 198*, 1474–1484. https://doi.org/10.1016/j.jclepro.2018.07.151

Sæther, M., Diehl, N., Monteiro, C., Li, H., Niedzwiedz, S., Burgunter-Delamare, B., Scheschonk, L., Bischof, K., & Forbord, S. (2024). The sugar kelp *Saccharina latissima* II: Recent advances in farming and applications. *Journal of Applied Phycology, 36*(4), 1953–1985. https://doi.org/10.1007/s10811-024-03213-1

Skjåk-Bræk, G., Murano, E., & Paoletti, S. (1989). Alginate as immobilization material. II: Determination of polyphenol contaminants by fluorescence spectroscopy, and evaluation of methods for their removal. *Biotechnology and Bioengineering, 33*(1), 90–94. https://doi.org/10.1002/bit.260330112

Smetacek, V., & Zingone, A. (2013). Green and golden seaweed tides on the rise. *Nature, 504*(7478), 84–88. https://doi.org/10.1038/nature12860

Tonon, T., Machado, C. B., Webber, M., Webber, D., Smith, J., Pilsbury, A., Cicéron, F., Herrera-Rodriguez, L., Jimenez, E. M., Suarez, J. V., Ahearn, M., Gonzalez, F., & Allen, M. J. (2022). Biochemical and elemental composition of pelagic *Sargassum* biomass harvested across the Caribbean. *Phycology, 2*(1), 204–215. https://doi.org/10.3390/phycology2010011

Torres, M. R., Sousa, A. P. A., Filho, E. A. T. S., Melo, D. F., Feitosa, J. P. A., Paula, R. C. M.d., & Lima, M. G. S. (2007). Extraction and physicochemical characterization of *Sargassum vulgare* alginate from Brazil. *Carbohydrate Research, 342*(14), 2067–2074. https://doi.org/10.1016/j.carres.2007.05.022

Tsikrika, K., Walsh, D., Joseph, A., Burgess, C. M., & Rai, D. K. (2021). High-pressure processing and ultrasonication of minimally processed potatoes: Effect on the colour, microbial counts, and bioactive compounds. *Molecules, 26*(9). https://doi.org/10.3390/molecules26092614

Vázquez-Delfín, E., Freile-Pelegrín, Y., Salazar-Garibay, A., Serviere-Zaragoza, E., Méndez-Rodríguez, L. C., & Robledo, D. (2021). Species composition and chemical characterization of *Sargassum* influx at six different locations along the Mexican Caribbean coast. *The Science of the Total Environment, 795*, Article 148852. https://doi.org/10.1016/j.scitotenv.2021.148852

Wardhani, D. H., Aryanti, N., Aziz, A., Firdhaus, R. A., & Ulya, H. N. (2021). Ultrasonic degradation of alginate: A matrix for iron encapsulation using gelation. *Food Bioscience, 41*, Article 100803. https://doi.org/10.1016/j.fbio.2020.100803

WHO. (2011). Evaluation of certain food additives and contaminants: Seventy-third report of the Joint FAO/WHO Expert Committee on Food Additives. https://www.who.int/publications/i/item/9789241209601.

Wu, M., Xu, Y., Niu, S., Zhang, S., Ren, X., Yang, D., Ma, Y., Dabbour, M., Mintah, B. K., He, R., & Li, H. (2025). Use of sonication and sodium alginate to synergistically modify milk proteins: Network reinforcement mechanism for shelf-stable ambient-temperature-storage yogurt. *International Journal of Biological Macromolecules, 332*, Article 148569. https://doi.org/10.1016/j.ijbiomac.2025.148569

Yang, X., Sui, H., Liang, H., Li, J., & Li, B. (2022). Effects of M/G ratios of sodium alginate on physicochemical stability and calcium release behavior of pickering emulsion stabilized by calcium carbonate. *Frontiers in Nutrition, 8*. https://doi.org/10.3389/fnut.2021.818290, 2021.

Yao, H.-Y.-Y., Wang, J.-Q., Yin, J.-Y., Nie, S.-P., & Xie, M.-Y. (2021). A review of NMR analysis in polysaccharide structure and conformation: Progress, challenge and perspective. *Food Research International, 143*, Article 110290. https://doi.org/10.1016/j.foodres.2021.110290

Yuan, Y., & Macquarrie, D. J. (2015). Microwave assisted step-by-step process for the production of fucoidan, alginate sodium, sugars and biochar from *Ascophyllum nodosum* through a biorefinery concept. *Bioresource Technology, 198*, 819–827. https://doi.org/10.1016/j.biortech.2015.09.090

Zhang, X., Chen, J., Shao, X., Li, H., Jiang, Y., Zhang, Y., & Yang, D. (2023). Structural and physical properties of alginate pretreated by high-pressure homogenization. *Polymers, 15*(15), 3225. https://doi.org/10.3390/polym15153225

Zhang, Y., Purohit, A., Aghayev, Z., Wang, Y., Liang, J., Beykal, B., Luo, Y., & Qiao, M. (2025). Optimization and evaluation of a simplified green biorefinery for alginate extraction from sugar kelp (*Saccharina latissima*). *International Journal of Biological Macromolecules, 309*, Article 143147. https://doi.org/10.1016/j.ijbiomac.2025.143147